Design and Performance Analysis of Fuzzy Based Hybrid Controller for Grid Connected Solar-Battery Unified Power Quality Conditioner

Koganti Srilakshmi* ⓘD, Sravanthy Gaddameedhi* ⓘD, D. Teja Santhosh ** ⓘD

N. Yashaswini *** ⓘD, Nagaraju Valluri**** ⓘD , J. Ganesh Prasad Reddy ***** ⓘD, NMG Kumar ****** ⓘD, D. Anil Naik * ⓘD

*Department of Electrical Engineering, Sreenidhi Institute of Science and Technology, Hyderabad, India.

** Department of Computer Science and Engineering, CVR College of Engineering, Hyderabad, India

*** Department of Mechanical Engineering, Sreenidhi Institute of Science and Technology, Hyderabad, India

**** Department of Electronics and communication Engineering, Sreenidhi Institute of Science and Technology, Hyderabad, India

***** Department of Electrical and Electronics Engineering, Sree Vahini Institute of Science and Technology, Tiruvuru, India

****** Department of Electrical and Electronics Engineering, Sree Vidyanikethan College of Engineering, Tirupathi, India

(kogantisrilakshmi29@gmail.com, sravanthi314@gmail.com, tejasantoshd@gmail.com, yashaswininandu@gmail.com, vsgnraju@gmail.com, jgpreddy@gmail.com, nmgkumar@gmail.com, dharavathanil208@gmail.com)

‡
Corresponding Author: Koganti Srilakshmi, Sreenidhi Institute of Science and Technology, Tel: +91-8885851666, kogantisrilakshmi29@gmail.com.

Abstract: Nowadays, integration of the non-conventional energy sources like wind, tidal, solar etc into the grid is suggested in order to minimize the losses in the distribution network and to meet the demand. The arrival of the power electronics equipments to control the nonlinear loads has made an impact on the power quality. The unified power quality conditioner is a FACTS device with the back to back converters, coupled together with a DC-Link capacitor. This paper suggests an intelligent hybrid controller for the solar Photo-voltaic system and Battery storage system integrated UPQC. The proposed controller is the combination of Fuzzy Logic controller and integral sliding-mode controller. The synchronization of phases is created by self tuning filter in association with unit vector generation method (STF-UVGM) for the superior performance of UPQC during the unbalanced/ distorted supply voltages conditions. Therefore, the necessity of Phase-locked-loop, Low pass filters and High pass filters are eliminated. However, Self tuning filter is used for separating the Harmonic and Fundamental components. In addition, STF-UVGM was used for generation of synchronization phases of series and shunt filters. The prime objectives of the suggested fuzzy logic integral sliding mode hybrid controller (FLISMHC) are fast action to retain the DC-Link voltage to the constant value during load/ irradiation variations, diminish the harmonics in the current waveforms, power-factor enhancement, maximum mitigation of sag/swell/ disturbances in the supply voltage, and appropriate compensation for the un-balanced supply voltages. The performance analysis of FLISMHC was investigated on five test cases for several combinations of loads/ supply voltages and to demonstrate the supremacy of the suggested FLISMHC comparative analysis was carried out with the methods that exist in literature and with the standard controllers like PI, sliding mode, and FL. The proposed method shows an extra-ordinary performance in diminishing THD thereby improving PF and reducing voltage distortions.

Keywords- Self tuning filter, Fuzzy-Logic controller, Unified Power Quality Conditioner, Solar PV generation, Battery system

Nomenclature:

			c phases
SUAPF	Shunt active filter	$V^{ref}_{se\_d}, V^{ref}_{se\_q}$	Series injected reference voltage in d - q domain
SEAPF	Series active filter	$V^{ref}_{se\_\alpha}, V^{ref}_{se\_\beta}$	Series injected reference voltage in α - β domain
PQ	Power-Quality		
UPQC	Unified Power Quality Conditioner	$V^{ref}_{\alpha}, V^{ref}_{\beta}$	Reference voltage in α - β domain
SPV	Solar Photo-Voltaic		
BS	Battery Storage	V^{ref}_{d}, V^{ref}_{q}	Reference voltage in d - q domain
FLC	Fuzzy Logic Controller		
PI	Proportional Integral	$i_{l\_a}, i_{l\_b}, i_{l\_c}$	Load current for a-b-c phase
SMC	Sliding-mode Control		
ISMC	Integral Sliding-mode Controller	$i_{l\_\alpha}, i_{l\_\beta}, i_{l\_0}$	Load currents in α - β - 0 domain
SYP	Synchronization of Phases	$i'_{l\_\alpha}, i'_{l\_\beta}, i'_{l\_0}$	FC of load currents in α - β - 0 domain
STF	Self Tuning Filter		
SMC	Sliding mode control	$i''_{l\_\alpha}, i''_{l\_\beta}, i''_{l\_0}$	HC of load current in α - β - 0 domain
UVGM	Unit Vector Generation Method	i''_{l_d}, i''_{l_q}	HC of loadcurrent in d - q domains
PLL	Phase-Locked-Loop		
LPFs	Low-Pass Filters	$i^{ref}_{l\_a}, i^{ref}_{l\_b}, i^{ref}_{l\_c}$	Reference load current for phases abc
HPFs	High-Pass Filters	$i^{ref}_{l\_\alpha}, i^{ref}_{l\_\beta}, i^{ref}_{l\_0}$	Reference load current α - β - 0 domain
FC	Fundamental-Component		
HC	Harmonic-Component	$i^{ref}_{l\_d}, i^{ref}_{l\_q}$	Reference load current in d - q domain
PF	Power Factor		
IOT	Internet of Things	$i_{sh\_a}, i_{sh\_b}, i_{sh\_c}$	SUAPF injected current for a-b-c phases
DSTATCOM	Distributed static compensator	$i^{ref}_{sh\_a}, i^{ref}_{sh\_b}, i^{ref}_{sh\_c}$	Reference SUAPF injected current for a-b-c phases
$V_{S\_a}, V_{S\_b}, V_{S\_c}$	Source voltage for a-b-c phases	$i_{sh\_a}, i_{sh\_b}, i_{sh\_c}$	SUAPF injected current for a-b-c phases
$i_{S\_a}, i_{S\_b}, i_{S\_c}$	Source current for a-b-c phases	C_{sh}	SUAPF Capacitance
$V_{S\_\alpha}, V_{S\_\beta}, V_{S\_0}$	Source voltage in α - β - 0 domain	R_{sh}	SUAPF Resistance
		L_{sh}	SUAPF Inductance
$V'_{S\_\alpha}, V'_{S\_\beta}, V'_{S\_0}$	FC of source voltage in α - β - 0 domain	C_{dc}	Capacitance of the capacitor across DC-Link
R_S	Source Resistance	V_{dc}	Actual voltage of DC-Link capacitor
L_S	Source Inductance		
$V_{l\_a}, V_{l\_b}, V_{l\_c}$	Load voltage for a-b-c phases	V^{ref}_{dc}	Reference voltage of DC-Link capacitor
$V_{se\_a}, V_{se\_b}, V_{se\_c}$	Series injected voltage for a-b-c phases	Δi_{dc}	DC-Link output error
$V^{ref}_{a}, V^{ref}_{b}, V^{ref}_{c}$	Reference voltages for a-b-	P_{PV}	Solar PV output power

V_{PV}	Solar output voltage
I_{PV}	Solar output current
$P_{DC-Link}$	Power at DC-Link
P_{BS}	Battery Power
V_{BS}	Battery voltage
i_{BS}	Battery current
Q	Battery capacity
DPD	DC-Link power demand
MF	Membership Functions
E	Error
CE	Change in error
SRFT	Synchronous Reference-Frame Theory
BC	Boost Converter
BBC	Buck-Boost Converter
$SOCB$	State of charge of Battery
SPG	Solar Power Generated

1. Introduction

Nowadays, distribution network is prone to PQ issues like interruptions, disturbances, flicker, sag/swell, and harmonics, PF etc due to the integration of inconsistent behavior wind, tidal, solar etc, the large non linear and unbalanced loads with power electronic equipments. However, this increased usage of the large non-liner industrial-loads leads to the decline in PF. Therefore, maintain of PQ has become the primary challenge to the power Engineers. The various configurations of single and /three phase SUAPF with various control techniques was suggested for three and four wire distribution systems for balanced and unbalanced supply voltages circumstances to attend PQ issues. In addition, the most recent developments and applications of SUAPF were also discussed [1]. The novel controller based on SRFT was designed for the 3φ-4wire UPQC to address the PQ issues effectively for both the un-balanced/ distorted loads of distribution system [2]. A hybrid controller with the combination of both FL and PI properties was developed for SUAPF with an aim of reducing THD to within the standards. To show the superiority of the proposed controller case study analysis was done for balanced and/ unbalanced loads [3]. Besides, the STF based solar battery connected SUAPF was developed in view of regulating the reactive power and minimizing current harmonics efficiently. While, to generate appropriate reference current the Maxikalman filter was introduced [4]. Further, the improvement in the intelligent based controllers like FL, ANN etc for SUAPF were able to addresses PQ problems effectively even for the dynamic load changes [5-7].

The solar integrated UPQC was developed and ability was tested on different load variations through the maximum power tracking with an aim of diminishing THD and boosting the overall performance of UPQC [8]. Besides, the SRFT based PI controller was designed for the fuel cell supported SUAPF with a goal of suppressing the current harmonics effectively and to regulate the voltage across DC-Link [9]. A new controller inspired by metaheuristic PSO and Grey Wolf Optimization based algorithms was suggested for the optimal tuning of SUAPF with the target of managing the reactive power and minimizing the THD efficiently [10]. However, to regulate the voltage and to control the reactive power at the grid a feed forward training based ANN controller was implemented on wind/solar associated UPQC [11]. A new adaptive control procedure was applied on the H-bridge UPQC with 8-switchs with a goal of minimizing THD and supply voltage distortions efficiently [12]. Besides, a multilevel UPQC associated with the PV/ wind and fuel cell was projected with an aim of eliminating voltage distortions and current harmonics efficiently [13]. The UPQC was recommended in order to suppress the current/ voltage harmonics for furnace load at steel power plant. However, to prove its superior performance comparative analysis was carried out with DSATCOM [14]. The development of efficient controller from the hybridization of both the properties of ANN, FL was carried out for the solar PV integrated UPQC to address the PQ problems and to show the viability of the proposed controller performance investigation was carried out for various combinations of the loads/ supply voltage conditions [15].

The Fourier-Transform was recommended for solar/ Wind/ Fuel-cell, and Battery connected UPQC with an aim of eliminating voltage distortions in the supply voltage and reducing imperfections in load current [16]. UPQC was employed to eliminate the voltage imbalances and to reduce imperfections in current harmonics by adaptive neuro-fuzzy hybrid controller in addition to the improvement in the utilization of network [17]. The FL controller was suggested for series active power filter for the grid connected distribution network to attend the PQ problems like voltage imperfections, current harmonics, and maintain DC-Link capacitor voltage [18]. A neuro-fuzzy interface hybrid controller was suggested for STF based wind battery integrated shunt active power filter to address PQ issues [19]. The benefits and challenges of integrating the renewable energy sources into the grid and their control strategies was studied [20]. The effects on the smart grid technologies on the national grid were highlighted and few suggestions were also given to convert conventional grid into smart grid [21]. The comparison between P & O and PSO algorithms to get MPP for the PV system was studied for solar irradiation changes [22]. Experimental set-up of isolated boost full bridge DC-DC converter was investigated along with a set of low loss active snubber circuit [23]. Integration of renewable sources to micro grid for MPPT was studies with power management [24]. High voltage isolated ACDC converters

were developed based on the modular technology [25]. FDNE based method was developed based on online least square identification algorithm along with digital simulators [26]. Fuzzy logic controller was suggested for PV-MPPT to improve the overall performance by maximum power point tracking [27]. A soccer league algorithm based optimal tuning of PI controller for UPQC was proposed to address the voltage and current PQ issues effectively [28]. Soccer league algorithm based optimal design of ANN controller was proposed to solar battery integrated UPQC to address power quality issues of distribution network [29].

Fig.1. Components of U-SPBS

Although many of controllers were developed, still there exists a scope for developing a new hybrid controllers and intelligent techniques for efficiently handling the PQ related issues. In this paper, a hybrid controller with the combination of FL and ISMC properties was designed for UPQC connected to SPV and BS systems (U-SPBS) with the objective of diminishing the current THD thereby enhancing PF, regulating the DC-Link voltage during load/solar irradiation variations, compensation during with sag/swell and disturbance condition. The STF-UVGM was suggested to generate synchronize phases for both series and shunt active power filters instead of PLL. However, STF also eliminates low pass and high pass filters for separating the fundamental and harmonic components of current. The performance analysis of the proposed controller for U-SPBS system was carried out for five different test cases, and to exhibit its supremacy comparative study was done with the conventional PI, SMC, FLC and other controllers that exist in literature. Section-2 gives the construction of proposed U-SPBS, section-3 provides the design of the proposed controller, Section-4 presents discussion of results, and section-5 is the Conclusion.

2. Construction of Proposed U-SPBS

The configuration of the proposed U-SPBS is shown in Fig.1. The SPV and BS are integrated to UPQC through a DC-link via a BC, and BBC. This paper designs a fuzzy based hybrid controller FLISMHC to exploit both the unique properties of FL and ISMC controllers. The UPQC is the arrangement of both the series and shunt converters. The role of SEAPF is to mitigate voltage related distortions like sags/ swell/disturbance, supply voltage unbalances. Beside, the isolation between Series converter and the power line are provided through injecting transformers. In addition, it injects suitable V_{se} into the grid. Similarly, the main objective of SUAPF is to suppress the harmonics in current waveform by injecting suitable i_{sh} and fast response to maintain the constant DC-link voltage across the capacitor. The 3φ balanced /unbalanced R-L loads, induction furnace load were considered in this work.

Table 1: Solar-PV Panel and Battery Ratings

Device	Parameters	Values
Solar-PV panel (SPR-215-WHT-U)	Output-power	214.92W
	Open circuit voltage	48.3V
	Short-circuit current	5.8A
	Maximum Voltage/current	39.80 V /5.40A
	No of PV cells connected in parallel	11
Li-ion battery	Rated Capacity	350 Ah
	Maximum capacity	450 Ah
	Normal-Voltage	650 V
	Full voltage	756 V

2.1 SPV System

The SPV and BS acts as exterior support for the DC-Link of UPQC, through a BC and BBC in a view of maintaining the stable voltage across the DC-Link capacitor during load variations, and minimizing of converter ratings as shown in Fig. 2. The SPV and BS ratings considered in this work are listed in Table 1. The power distribution of U-SPBS at the DC link is given by Eq. (1).

$$P_{PV} + P_{BS} - P_{DC-Link} = 0 \qquad (1)$$

2.2 BS System

BS controller contains a lead-acid type of battery connected to BBC. It provides the stable voltage across the DC-Link as given in Fig. 2. $SOCB$ is calculated by Eq. (2).

$$SOCB = 100\,(1 + \int i_{BS}\ dtQ) \qquad (2)$$

The amount of power generated by the SPV will decides the state of operation of a battery: charging or discharging by satisfying the upper and lower constraints given by Eq. (3).

$$SOCB_{min} \le SOCB \le SOCB_{max} \quad (3)$$

The DC-link's reference current $i^{ref}{}_{dc}$ is estimated by minimizing the error of DC-Link's voltage $V_{dc,error}$ by a PI-controller. The reference error current of the battery $i_{BS,error}{}^{*}$ is calculated by PI controller through a battery's error current $i_{BS,error}$. Where, $i_{BS,error}$ is difference between reference DC-Link current $i^{ref}{}_{dc}$ and battery current $i^{ref}{}_{BS}$ obtained from LPF. K_{p1} =0.7, K_{i1} =10.1, K_{p2} =2.77 and K_{i2} = 11.17 gains are taken arbitrarily.
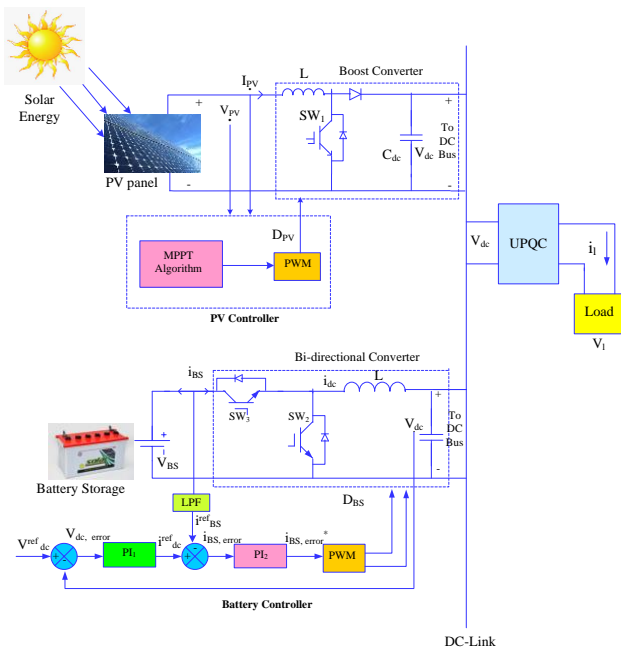
Fig.2. Proposed UPQC with SPV and BS Controllers

Table 2 provides the power distribution across the DC-link under various levels of SPG.

Table 2. Power-sharing at DC-link

Intensity of SPG	Action
$SPG > P_{dc}$	Excess SPG is utilized to charge Battery till it attains $SOCB_{max}$
$SPG = P_{dc}$	SPG alone will supply P_{dc}.
$SPG < P_{dc}$	The difference power is provided by Battery until it attains $SOCB_{min}$.
Nill SPG	Only BS supplies P_{dc}.

3. Control Strategy of U-SPBS using STF

During the fault or change in load, the voltage across capacitor of the DC-link varies. So, it is very important to make DC-Link voltage stable within a short duration of time. In d-q theory, first currents and voltages are transformed into the clarke's reference. In general, the conventional UPQC mechanism consists of SUAPF, SEAPF and PLL. In this proposed system STF- UVGM is used to generate SYP from the distorted supply voltages and also performs the role of PLL, HPFs and LPFs for separating the FC/ HC of currents. So, the suggested system consists of a STF, SUAPF and a SEAPF. The switching of series and shunt VSCs are carried out with the PWM voltage and PWM hysteresis current controllers with FLISMHC. As the design of STF is already available in the literature the major parts of the proposed controlling structure are given below:

3.1 STF-UVGM

The suggested STF-UVGM is non-iterative method which provides SYP from the supply voltage as shown in Fig. 4- 5. In Eq. 4 the Clarke's domain is used to transform the supply voltage from abc to $\alpha\beta0$ domain.

$$\begin{bmatrix} V_{S\_\alpha} \\ V_{S\_\beta} \\ V_{S\_0} \end{bmatrix} = \sqrt{\frac{2}{3}} \begin{bmatrix} 1 & -\frac{1}{2} & -\frac{1}{2} \\ 0 & \frac{\sqrt{3}}{2} & -\frac{\sqrt{3}}{2} \\ \frac{1}{2} & \frac{1}{2} & \frac{1}{2} \end{bmatrix} \begin{bmatrix} V_{S\_a} \\ V_{S\_b} \\ V_{S\_c} \end{bmatrix} \qquad (4)$$

The FC and HC are separated from the distorted grid voltages as given in Eq. 5 by considering only $\alpha\beta$ domain.

$$\begin{bmatrix} V_{S\_\alpha} \\ V_{S\_\beta} \end{bmatrix} = \begin{bmatrix} V'_{S\_\alpha} + V''_{S\_\alpha} \\ V'_{S\_\beta} + V''_{S\_\beta} \end{bmatrix} \qquad (5)$$

Here, V'_{S_α} indicates the FC and V''_{S_α} indicates the HC in $\alpha\beta$ domain. The STF suppress the HC in the distorted grid voltages and extracts the FC to produce SYP with high quality. The Laplace transformation of STF is expressed by Eq. 6.

$$\begin{bmatrix} V'_{S\_\alpha}(s) \\ V'_{S\_\beta}(s) \end{bmatrix} = \frac{k1}{s}\begin{bmatrix} V_{S\_\alpha}(s) - V'_{S\_\alpha}(s) \\ V_{S\_\beta}(s) + V'_{S\_\beta}(s) \end{bmatrix} + \frac{2\pi f c1}{s}\begin{bmatrix} V'_{S\_\beta}(s) \\ -V'_{S\_\alpha}(s) \end{bmatrix} \quad (6)$$

Where, k_1 is the gain selected as 20 and f_{c1} is the cut-off-frequency whose value is similar to the systems frequency 50Hz. The SYP $\sin(wt)$ and $\cos(wt)$ are generated from Eq. 7 which omits PLL. STF-UVGM effectively generates SYP for distorted supply voltage of U-SPBS.

$$\begin{bmatrix} \sin(wt) \\ \cos(wt) \end{bmatrix} = \frac{1}{\sqrt{\left(V'_{S\_\alpha}\right)^2 + \left(V'_{S\_\beta}\right)^2}}\begin{bmatrix} V'_{S\_\alpha} \\ -V'_{S\_\beta} \end{bmatrix} \quad (7)$$

3.2 Shunt Controller

The main function of SUAPF is to suppress the current harmonics by injecting required amount of current, and to regulate DC capacitor voltage stable. The shunt-controller adapts (i) abc - $\alpha\beta0$, $\alpha\beta0$ - dq, dq - $\alpha\beta0$, and $\alpha\beta0$ - abc transformations; (ii) FLISMHC is applied for minimizing the THD and regulating the DC-link voltage. The proposed method compares the actual voltage of DC link with the reference voltage and transfers the error (current output) into the axis. The proposed controller is given in Fig. 3. The transformations of domains along with the STF, the design of controller is given below:
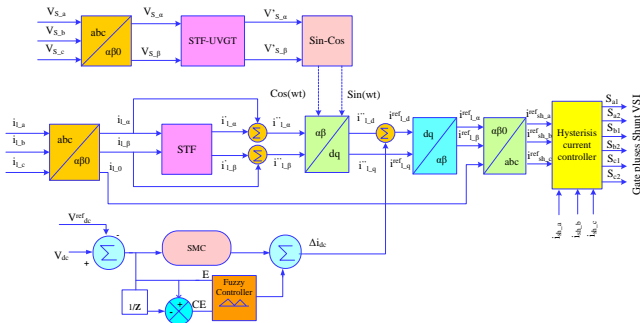
Fig.3. FLISMHC for Shunt Converter

In SUAPF initially, the load currents are shifted to α - β - 0 coordinates by using clarke transformation adopting Eq.8.

$$\begin{bmatrix} i_{l\_\alpha} \\ i_{l\_\beta} \\ i_{l\_0} \end{bmatrix} = \sqrt{\frac{2}{3}}\begin{bmatrix} 1 & -\dfrac{1}{2} & -\dfrac{1}{2} \\ 0 & \dfrac{\sqrt{3}}{2} & -\dfrac{\sqrt{3}}{2} \\ \dfrac{1}{2} & \dfrac{1}{2} & \dfrac{1}{2} \end{bmatrix}\begin{bmatrix} i_{l\_a} \\ i_{l\_b} \\ i_{l\_c} \end{bmatrix} \quad (8)$$

By performing the Laplace conversion the STF splits the HC from the FC by the given in Eq. 9.

$$\begin{bmatrix} i'_{l\_\alpha}(s) \\ i'_{l\_\beta}(s) \end{bmatrix} = \frac{k2}{s}\begin{bmatrix} i_{l\_\alpha}(s) - i'_{l\_\alpha}(s) \\ i_{l\_\beta}(s) + i'_{l\_\beta}(s) \end{bmatrix} + \frac{2\pi f c2}{s}\begin{bmatrix} i'_{l\_\beta}(s) \\ -i'_{l\_\alpha}(s) \end{bmatrix} \quad (9)$$

Where, k_2 is the gain= 20 and f_{c2} is the cut-off-frequency = 50Hz system frequency. The HC in α - β - 0 coordinates are obtained by Eq. 10.

$$\begin{aligned} i''_{l\_\alpha} &= i_{l\_\alpha} - i'_{l\_\alpha} \\ i''_{l\_\beta} &= i_{l\_\beta} - i'_{l\_\beta} \end{aligned} \quad (10)$$

$$\begin{aligned} i''_{l\_d} &= i''_{l\_\alpha}\sin(wt) - i''_{l\_\alpha}\cos(wt) \\ i_{l\_q} &= i_{l\_\alpha}\cos(wt) + i_{l\_\beta}\sin(wt) \end{aligned} \quad (11)$$

By the use of HC from Eq. 10 and SYP from Eq. 11 the HC in d-frame is obtained. The reference current generation and stable DC-Link voltage plays a vital role in determining the performance of the SUAPF. However, if load changes the active power flow in the SUAPF may vary which leads to voltage instable across DC-Link. So, in order to regulate the voltage across the DC link the active power in SUAPF is made equal to the switching losses. The suggested FLISMHC injects an appropriate error current signal Δi_{dc}. The mathematical expression for the calculation of DC-Link voltage is given by Eq. 12.

$$E(t) = V^{ref}{}_{dc} - V_{dc}(t) \quad (12)$$

Where, $k_{p,sh}$ and $k_{i,sh}$ are chosen as 0.3 and 2 respectively. The reference load current in d-axis can be calculated in Eq. 13.

$$i^{ref}{}_{l\_d} = i''_{l\_d} - \Delta i_{dc} \quad (13)$$

The d - q reference load currents are transformed into α - β domain by applying Eq. 14. Later, the reference shunt injected currents are transformed into abc domain by Eq. 15.

$$\begin{bmatrix} i^{ref}{}_{l\_\alpha} \\ i^{ref}{}_{l\_\beta} \end{bmatrix} = \begin{bmatrix} \sin(wt) & \cos(wt) \\ -\cos(wt) & \sin(wt) \end{bmatrix}\begin{bmatrix} i^{ref}{}_{l\_d} \\ i^{ref}{}_{l\_q} \end{bmatrix} \quad (14)$$

$$\begin{bmatrix} i_{sh}{}^{ref}{}_{\_a} \\ i_{sh}{}^{ref}{}_{\_b} \\ i_{sh}{}^{ref}{}_{\_c} \end{bmatrix} = \sqrt{\frac{2}{3}}\begin{bmatrix} 1 & 0 \\ -\dfrac{1}{2} & \dfrac{\sqrt{3}}{2} \\ -\dfrac{1}{2} & -\dfrac{\sqrt{3}}{2} \end{bmatrix}\begin{bmatrix} i^{ref}{}_{l\_\alpha} \\ i^{ref}{}_{l\_\beta} \end{bmatrix} \quad (15)$$

The errors currents obtained from the comparison of the actual and reference signals are transferred to a hysteresis control in order to produce appropriate gating pulses.

3.2.1 Proposed FLISMHC

The FLC is an intelligent controller which functions on the linguistic rules. The main components of an FLC system are a fuzzifier, a rule base, knowledge base, an inference, and a defuzzifier. The fuzzzifier converts numerical inputs into linguistic variables with the support of MF. The knowledge base stores the updated information about all the input-output relationships. Then, inference determines the rule base and MF of the fuzzy. Lastly, defuzzifier coverts fuzzy variables to crisp output. The flow of FLC is illustrated in Fig.4. The Takagi Sugeno scheme is applied for the proposed work; it takes E and CE as inputs to the system. Where, E is obtained from the Eq.16. The fuzzy variables are represented by triangular MF as shown in Fig. 5-7 involving HP, medium positive (MP), LP, Zero (ZO), HN, medium negative (MN) and LN. The DC Link voltage values are considered in the range of these linguistic terms with 49 sets of MFs as given in Table 3.

$$E = V^{ref}{}_{dc} - V^{i}{}_{dc} ; i = 1,2,3,4,5,6 \quad (16)$$
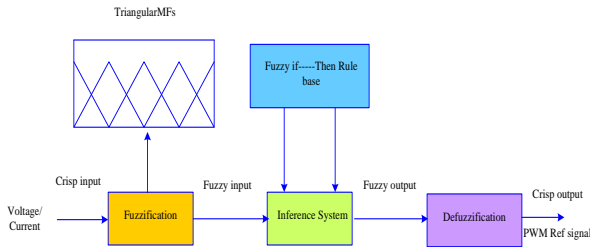
Fig. 4. Process of Fuzzy Logic

ISMC is a non-linear controller generally used to control non-linear behavior power electronic FACTS devices. The major role of ISMC is the surface specification, generally called as a sliding-surface. The prime feature is to regulate the system within its surface. The main steps involved in ISMC controllers are highlighted below 1) Sliding-surface suggestion, 2) Identification of presence of SM surface, and 3) Stability analyses of the surface.
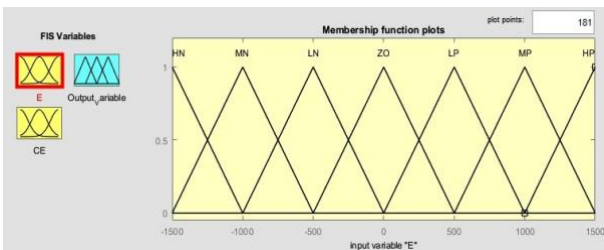
Fig.5. MF of "E"
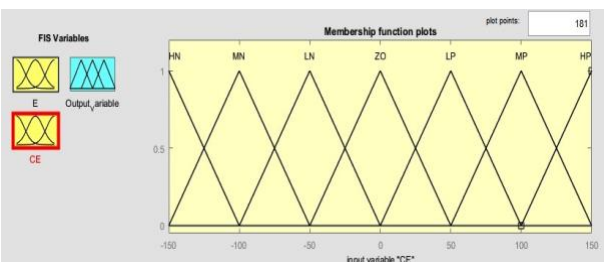
Fig.6. MF of "CE"
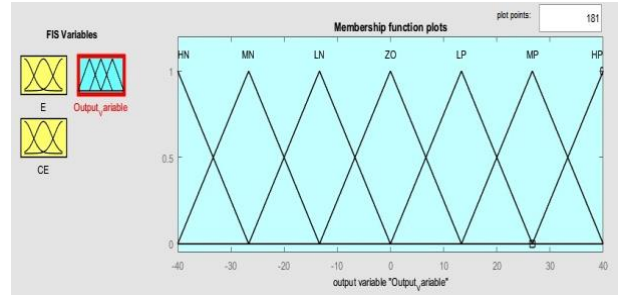
Fig.7. MF of "Output duty cycle"

Table 3. MF mapping for voltage across DC-link

Er	CE						
	HP	MP	LP	ZO	LN	MN	HN
HN	ZO	LN	MN	HN	HN	HN	HN
MN	LP	ZO	LN	MN	HN	HN	HN
LN	MP	LP	ZO	LN	MN	HN	HN
ZO	HP	MP	LP	ZO	LN	MN	HN
LP	HP	HP	MP	LP	ZO	LN	MN
MP	HP	HP	HP	MP	LP	ZO	LN
HP	HP	HP	HP	HP	MP	LP	ZO

The error $e(n)$ is evaluated by Eq. (17).

$$x_1 = V^{ref}{}_{dc} - V_{dc} = e(n) \quad (17)$$

The derivative of the calculated error is obtained by Eq.(18).

$$x_2 = \frac{1}{T} e(n) - e(n-1) \quad (18)$$

Where, T is interval of time, and x_1 and x_2 are state space variables whose equation is given by Eq. (19)

$$\dot{x} = \begin{bmatrix} \dot{x_1} \\ \dot{x_2} \end{bmatrix} = \begin{bmatrix} 0 & 1 \\ 0 & 0 \end{bmatrix} \begin{bmatrix} x_1 \\ x_2 \end{bmatrix} + \begin{bmatrix} 0 \\ -k \end{bmatrix} \mu \quad (19)$$

The state space equation of sliding plane is represented by Eq. (20) and (21) respectively.

$$s = \begin{bmatrix} C & 1 \end{bmatrix} \begin{bmatrix} x_1 \\ x_2 \end{bmatrix} = Cx_1 + x_2 \quad (20)$$

$$\dot{s} = \begin{bmatrix} C & 1 \end{bmatrix} \begin{bmatrix} \dot{x_1} \\ \dot{x_2} \end{bmatrix} = C\dot{x_1} + \dot{x_2} \quad (21)$$

Power rate reaching law is given as,

$$\dot{s} = -L|s|^{\alpha} \operatorname{sgn}(s) \quad (22)$$

Where,

$$\text{sgn}(s) = \begin{Bmatrix} 1 \\ -1 \end{Bmatrix} \ for \ \begin{matrix} s > 0 \\ s < 0 \end{matrix} \tag{23}$$

The control law μ is calculated from Eqs. (24)

$$\mu = \frac{1}{K}\Big[Cx_2 + L|s|^\alpha \, \text{sgn}(s)\Big] \tag{24}$$

The control action is incorporated to get the modified control-law as given in Eq. (25).

$$\mu = \frac{1}{K}\Big[Cx_2 + L|s|^\alpha \, \text{sgn}(s)\Big] + K_i * \int_0^t e(\tau)d\tau \tag{25}$$

3.3 Series Controller

The main purpose of SEAPF is to eliminate voltage related PQ issues by injecting appropriate voltage through interfacing transformer. By using Eq.26 the source voltages are transferred into $\alpha - \beta - 0$ coordinates.

$$\begin{bmatrix} V_{S\_\alpha} \\ V_{S\_\beta} \\ V_{S\_0} \end{bmatrix} = \sqrt{\frac{2}{3}} \begin{bmatrix} 1 & -\dfrac{1}{2} & -\dfrac{1}{2} \\ 0 & \dfrac{\sqrt{3}}{2} & -\dfrac{\sqrt{3}}{2} \\ \dfrac{1}{2} & \dfrac{1}{2} & \dfrac{1}{2} \end{bmatrix} \begin{bmatrix} V_{S\_a} \\ V_{S\_b} \\ V_{S\_c} \end{bmatrix} \tag{26}$$
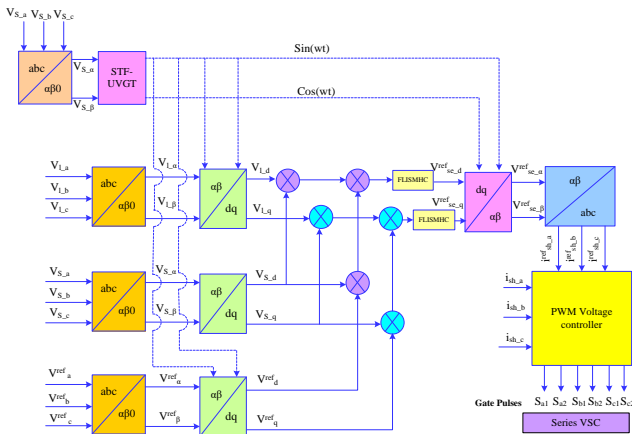
Fig.8. Series controller

$$\begin{bmatrix} V_{S\_d} \\ V_{S\_q} \end{bmatrix} = \begin{bmatrix} \cos(wt) & \sin(wt) \\ -\sin(wt) & \cos(wt) \end{bmatrix} \begin{bmatrix} V_{S\_\alpha} \\ V_{S\_\beta} \end{bmatrix} \tag{27}$$

The 3φ voltage is transformed into $d - q$ two phase using park conversion by using Eq. 27.

$$\begin{bmatrix} V_{l\_\alpha} \\ V_{l\_\beta} \\ V_{l\_0} \end{bmatrix} = \sqrt{\frac{2}{3}} \begin{bmatrix} 1 & -\dfrac{1}{2} & -\dfrac{1}{2} \\ 0 & \dfrac{\sqrt{3}}{2} & -\dfrac{\sqrt{3}}{2} \\ \dfrac{1}{2} & \dfrac{1}{2} & \dfrac{1}{2} \end{bmatrix} \begin{bmatrix} V_{l\_a} \\ V_{l\_b} \\ V_{l\_c} \end{bmatrix} \tag{28}$$

$$\begin{bmatrix} V_{l\_d} \\ V_{l\_q} \end{bmatrix} = \begin{bmatrix} \cos(wt) & \sin(wt) \\ -\sin(wt) & \cos(wt) \end{bmatrix} \begin{bmatrix} V_{l\_\alpha} \\ V_{l\_\beta} \end{bmatrix} \tag{29}$$

By using Eq.28 the load voltages are transferred into $\alpha - \beta - 0$ coordinates and to two phase $d - q$ domain by Eq. 29 by applying clark and park transformations.

$$\begin{bmatrix} V^{ref}_a \\ V^{ref}_b \\ V^{ref}_c \end{bmatrix} = V_{max} \begin{bmatrix} \sin(wt) \\ \sin(wt - 2\pi/3) \\ \sin(wt + 2\pi/3) \end{bmatrix} \tag{30}$$

$$\begin{bmatrix} V^{ref}_\alpha \\ V^{ref}_\beta \\ V^{ref}_0 \end{bmatrix} = \sqrt{\frac{2}{3}} \begin{bmatrix} 1 & -\dfrac{1}{2} & -\dfrac{1}{2} \\ 0 & \dfrac{\sqrt{3}}{2} & -\dfrac{\sqrt{3}}{2} \\ \dfrac{1}{2} & \dfrac{1}{2} & \dfrac{1}{2} \end{bmatrix} \begin{bmatrix} V^{ref}_a \\ V^{ref}_b \\ V^{ref}_c \end{bmatrix} \tag{31}$$

$$\begin{bmatrix} V^{ref}_d \\ V^{ref}_q \end{bmatrix} = \begin{bmatrix} \cos(wt) & \sin(wt) \\ -\sin(wt) & \cos(wt) \end{bmatrix} \begin{bmatrix} V^{ref}_\alpha \\ V^{ref}_\beta \end{bmatrix} \tag{32}$$

Similarly, reference voltage signal is calculated in abc by following Eq. 30 by applying STF-UVGM to obtain maximum peak voltage value V_{max} from the fundamental component. The load voltages are transformed into $\alpha - \beta - 0$ coordinates and to two phase $d - q$ domain by Eq. 31-32 by applying clark and park transformations.

$$V^{ref}_{se\_d} = \left(V^{ref}_d - V_{S\_d}\right) - \left(V_{l\_d} - V_{S\_d}\right)$$
$$V^{ref}_{se\_q} = \left(V^{ref}_q - V_{S\_q}\right) - \left(V_{l\_q} - V_{S\_q}\right) \tag{33}$$

$$\begin{bmatrix} V_{se\_\alpha} \\ V_{se\_\beta} \end{bmatrix} = \begin{bmatrix} \sin(wt) & \cos(wt) \\ -\cos(wt) & \sin(wt) \end{bmatrix} \begin{bmatrix} V^{ref}_{se\_d} \\ V^{ref}_{se\_q} \end{bmatrix} \tag{34}$$

$$\begin{bmatrix} V^{ref}_{se\_a} \\ V^{ref}_{se\_b} \\ V^{ref}_{se\_c} \end{bmatrix} = \sqrt{\frac{2}{3}} \begin{bmatrix} 1 & 0 \\ -\dfrac{1}{2} & \dfrac{\sqrt{3}}{2} \\ -\dfrac{1}{2} & -\dfrac{\sqrt{3}}{2} \end{bmatrix} \begin{bmatrix} V^{ref}_{se\_\alpha} \\ V^{ref}_{se\_\beta} \end{bmatrix} \tag{35}$$

The reference series injected voltage obtained from the difference between the actual reference source and load voltage demonstrated in Eq. 33-35. The injected series

voltage passes through the PWM voltage controller to generate the required pulses for of the SEAPF shown in Fig.8.

4. Simulation and Results

To analyze the performance efficiency of the suggested controller of U-SPBS a 3ω distribution system was selected. The U-SPBS and load specifications are exhibited in Table-4. Five test studies with multiple combinations of balanced/ unbalance/ non-liner loads, supply voltages, variable irradiation and conditions like swell/sag/disturbance with constant temperature of 25^0c was considered to attest the extraordinary performance of FLISMHC on proposed U-SPBS as shown in Table 5.

The V_S was considered to be balanced for case studies 1, 2 and un-balanced for 3, 4 and 5 respectively with various combinations of swell/ sag, disturbance voltages with variable irradiation and constant temperature conditions. In addition, the THD was obtained for i_S of the proposed system for all the case studies and further it is compared with those of PI/ SMC and /FL controllers. The PF is calculated from the THD by Eq. 36 for all considered case studies as given in Fig.9.

$$PF = \cos\theta * \frac{1}{\sqrt{1+THD^2}} \qquad (36)$$

Here, ө is the measured angle between voltage and current, while $\frac{1}{\sqrt{1+THD^2}}$ represents displacement factor.

Table 4. Ratings of U-SPBS

Source	V_s : 415V ; f : 50Hz R_s : 0.1 Ω ; L_s : 0.151 mH
SEAPF	R_{se} : 1 Ω ; L_{se} : 3.60 mH ; C_{se} : 60.0 μf
SUAPF	R_{sh} : 0.00101 Ω ; L_{sh} : 2.150 mh ; C_{sh} : 1.0 μF Hysteresisband: 0.01 A
DC link	C_{dc} : 9400 μf ; V_{dc} : 700 V

In case1, the supply voltage was considered to be balanced and sagged by 30% during the interval of 0.20-0.30 sec and swelled by 30% during 0.40-0.50 sec. In addition, disturbance was also introduced during the time period of 0.60-0.70 sec, as illustrated in Fig. 10(a). The waveform of load current was observed to be non-sinusoidal and balanced due to the nonlinear balanced rectifier-load is illustrated in Fig. 10(b). However, it clearly exhibits that the U-SPBS can eliminate voltage related and current related PQ issues effectively by injecting suitable compensating voltage and current. Such

improvement in the shapes of waveforms also reciprocated in the THD and power factor values. Therefore, the current THD was decreased from 20.54% to 2.40%, which is smaller when compared to those of other methods as given in Table 10 and the PF rose from 0.7144 to 0.9977 by injecting required series voltages and shunt currents. In addition, the suggested controller provides a stable DC-Link voltage during 1000W/m2 irradiation and constant temperature of 25^0c as shown in Fig. 10(c).

In case2, the supply voltage was considered to be balanced with the voltage related issues as similar to the case1, but irradiation of 800W/m2 as exhibited in Fig. 11(a). Here, the load current waveform was observed to be non-sinusoidal and un-balanced with a due to the non-linear balanced and unbalanced loads acting simultaneously as given in Fig. 11(b). It is clearly visible from the waveforms that the U-SPBS was able to voltage related PQ problems successfully and diminishes THD from 15.31% to 2.30% thereby boosting the PF value from 0.8552 to 0.9984 by injecting suitable compensating voltages and currents. However, as demonstrated in fig. 11(c) suggested controller works efficiently in maintaining constant voltage across DC-Link during load and irradiation variation simultaneously.

Table 5. Test cases considered under constant 25^0c temperature

Condition / Load	Case1	Case2	Case3	Case4	Case5
Balanced Supply Voltage	✓	✓			
Unbalanced Supply voltage			✓	✓	✓
Voltage swell/ sag/disturbance	✓	✓			
Steady state current	✓	✓	✓	✓	✓
Steady state voltage			✓	✓	✓
Irradiation 1000W/m2	✓		✓		✓
Irradiation 800W/m2		✓		✓	
Load1: Balanced-rectifier- 30.00Ω & 20.00mH	✓	✓	✓		✓
Load2: Unbalanced R-L- R: 10, 20 &15 ohm; L: 9.50 mH, 10.50 Mh & 18.50 mH.		✓		✓	
Load3: Induction-Furnace- LC = 400mh, 50Mf, RL = 10ohm,100mH					✓

In case3, the supply voltage was considered to be unbalanced for 3ωbalanced rectifier load with 1000W/m2 irradiation as given in Fig. 12(a). The load current was observed to be highly non-sinusoidal and balanced as in

Fig. 12(b). However, the FLISMHC was able to suppress the THD from 12.63% to 2.94%, improves PF from 0.7399 to 0.9977 and balances load voltage successfully by injecting suitable appropriate currents and voltages. In addition, it also stables DC-Link voltage as in Fig. 12(c).

In case4, the supply voltage and load both was considered to be unbalanced with 800W/ m2 given in Fig. 13(a). The load current waveforms are observed to be sinusoidal but unbalanced as shown in Fig. 13(b). The FLISMHC is able to suppress the harmonics in the current waveform and decreases THD from 19.63% to 4.16% while boosting up the PF from 0.6382 to 0.9983. Fig.13(c) exhibits its performance in regulating DC-Link voltage during load variation. Table 6 provides the comparison of proposed controller with the controllers that available in the literature.

In case5, the unbalanced supply voltage was considered with the combination of 3φ rectifier load and induction furnace loads with 1000W/m2 irradiation as illustrated in Fig. 14(a). The load current was balanced with non-sinusoidal structure as in Fig. 14(b). The suggested FLISMHC diminishes the THD from 26.12% to 3.42% and boosts up PF from 0.725 to 0.9922 effectively. However, the stable DC-link voltage was maintained as shown in Fig.14(c) during the dynamic variation in solar irradiation under constant temperature. Fig 15 shows the performance of the proposed controller in maintaining the constant DC-Link voltage during irradiation variation under constant temperature of 25^0c. The THD spectrum for all the proposed test studies is as given in Fig.16.

Table 6. % THD comparison of proposed controller with those of the available in literature

Controller	Case1	Case2	Case3	Case4	Case 5
Without UPQC	20.54	15.31	12.63	19.63	26.12
PI	4.97	5.68	4.25	5.02	5.23
SMC	4.74	3.74	4.23	4.09	4.26
FLC	4.01	3.43	3.14	4.14	4.17
PI [16]	3.28	--	--	--	--
SMC [16]	2.44	--	--	--	--
PI [17]	14.74	--	--	--	--
FLC [17]	6.13	--	--	--	--
ANFIS [17]	2.43	--	--	--	--
PI [18]	3.65	--	--	--	--
FLC [18]	2.52	--	--	--	--
FLISMHC	**2.40**	**2.30**	**2.94**	**4.16**	**3.42**
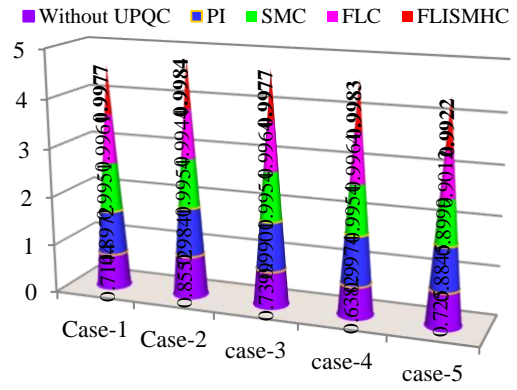
Fig.9. PF for test cases
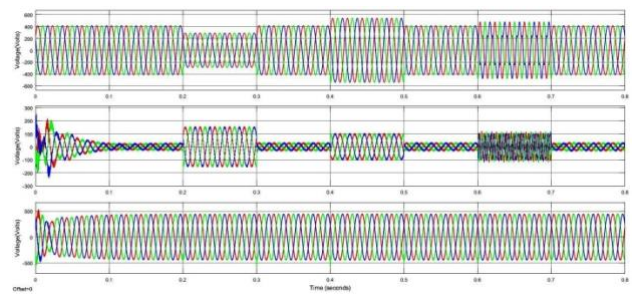
(a) V_S , V_{se} , V_l
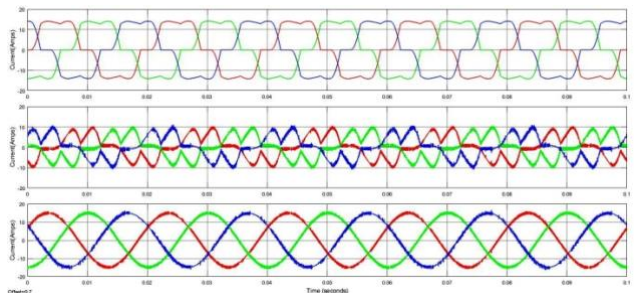
(b) i_l , i_{sh} , i_S
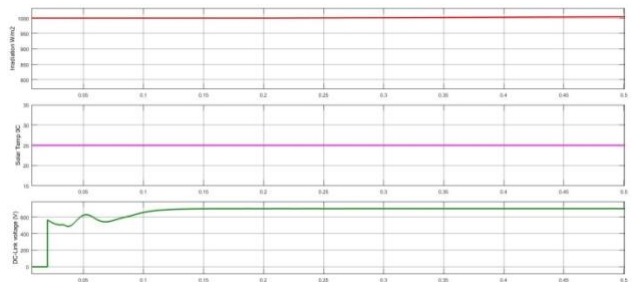
(C) Solar irradiation, temperature, DC-link voltage
Fig.10. Waveforms of U-SPBS for case-1
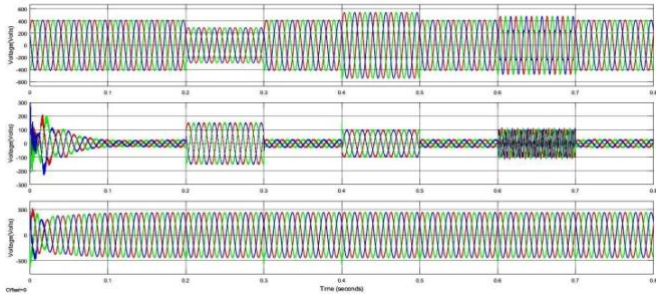
(a) V_S, V_{se}, V_l
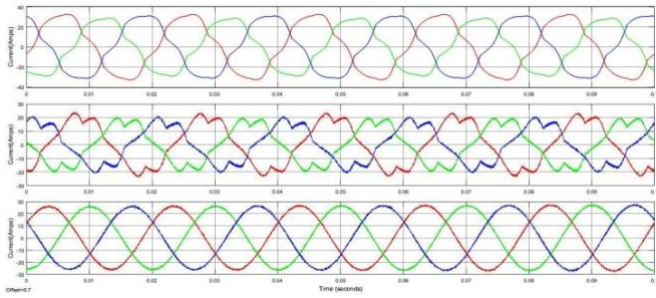
(b) i_l, i_{sh}, i_S
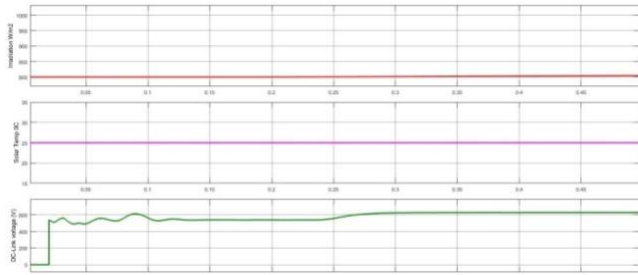
(c) Solar irradiation, temperature, DC-link voltage
Fig.11. Waveforms of U-SPBS for case-2
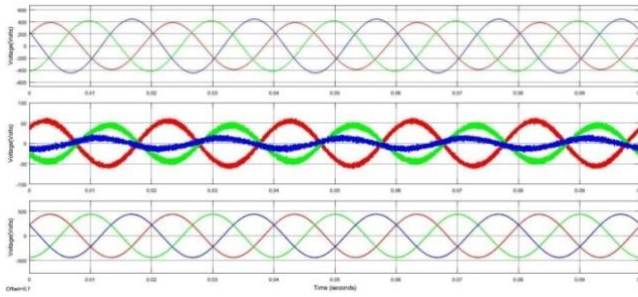
(a) V_S, V_{se}, V_l
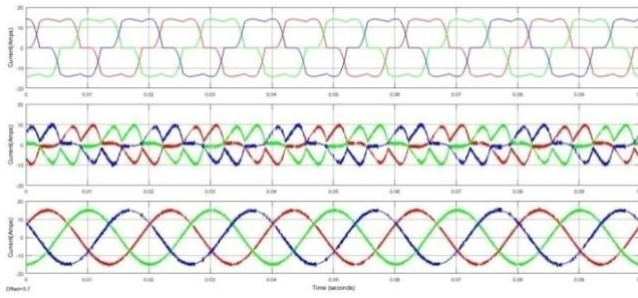
(b) i_l, i_{sh}, i_S
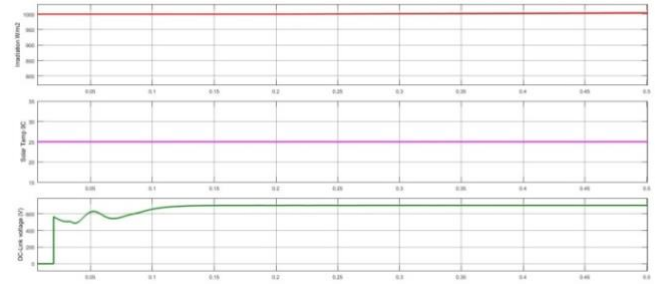
(c) Solar irradiation, temperature, DC-link voltage
Fig.12. Waveforms of U-SPBS for case-3
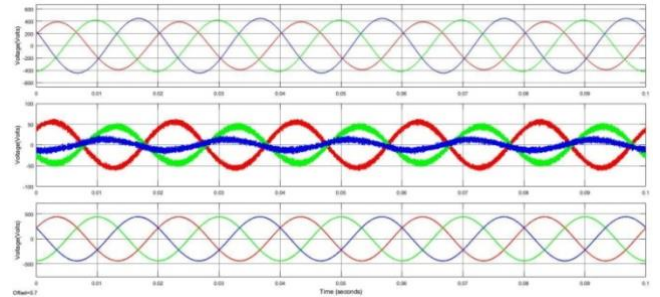
(a) V_S, V_{se}, V_l
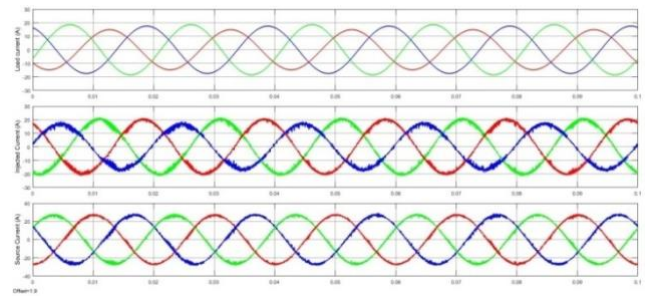
(b) i_l, i_{sh}, i_S
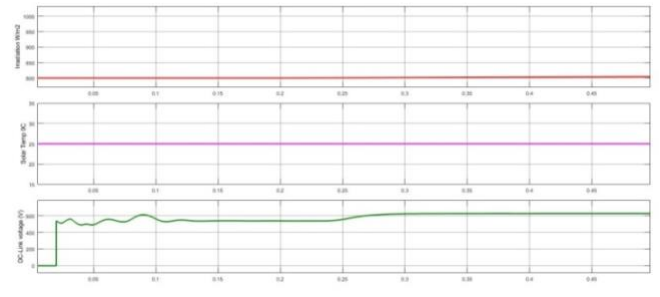
(c) Solar irradiation, temperature, DC-link voltage
Fig.13. Waveforms of U-SPBS for case-4

(a) V_S, V_{se}, V_l

11
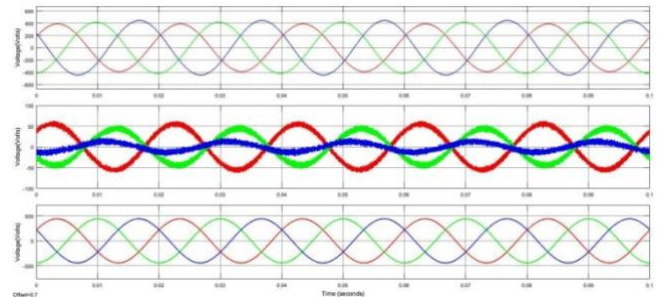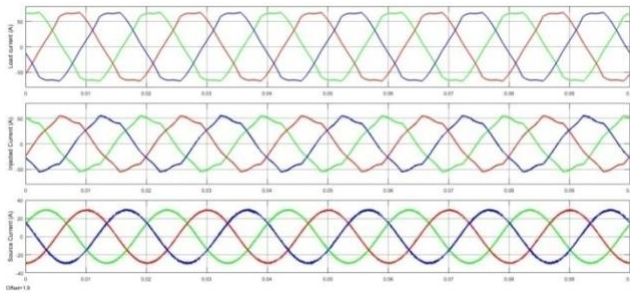
(b) i_l, i_{sh}, i_S
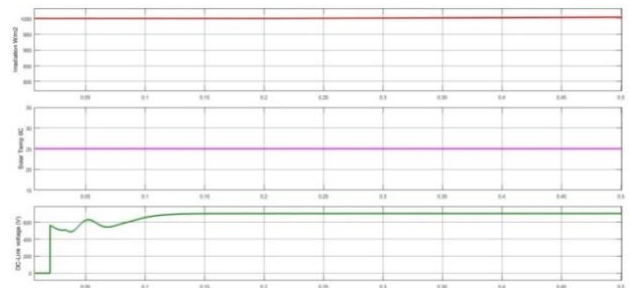
(c) Solar irradiation, temperature, DC-link voltage

Fig.14. Waveforms of U-SPBS for case-5
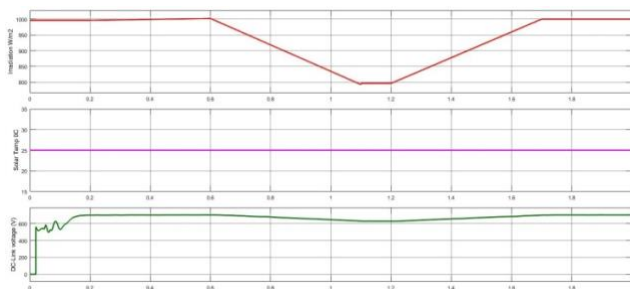
Fig.15. Waveforms for U-SPBS during (a) solar irradiation variation (b) 25^0c constant temperature (c) DC-Link voltage with settling time

Case-1

Case-2

Case-3

Case-4

Case-5
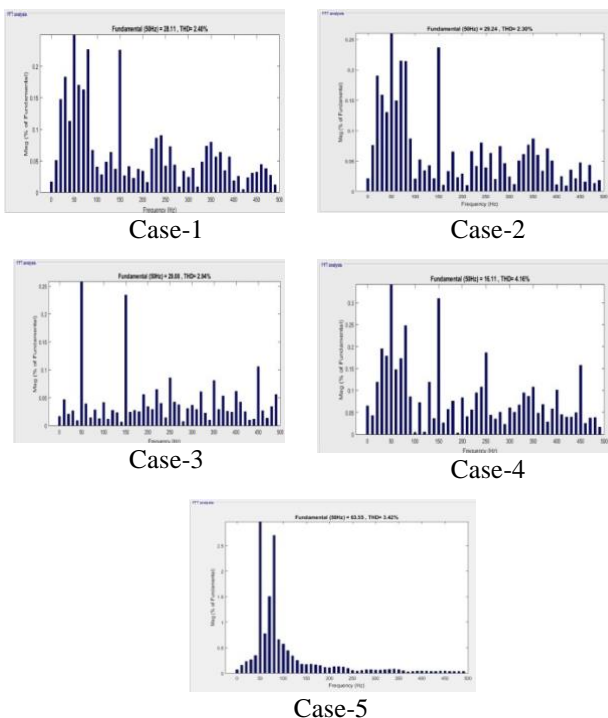
Fig.16. THD spectrum for case studies

5. Conclusion

The hybrid controller with the combination of FLC and ISMC properties are proposed for STF based U-SPBS. The design of controllers for SPV and BS were also specified in addition to the development of FLISMHC for shunt controller with an aim of quick stabilizing the DC-Link capacitance voltage, eliminating swell, sag, disturbances in supply voltage, suppressing the harmonics in source current, and boosting the PF. From the investigation on five test cases it is clearly exhibited that the FLISMHC was able to reduce the THDs within the acceptable limits of IEEE standards and improves PF to almost unity. Moreover, by the comparative analysis it has been proved that the performance was much better than those of the conventional controllers like PI, SMC and FLC and other controllers that exist in the literature. The FLISMHC also maintains the stable voltage across DC link constant during irradiation and load variations. The proposed system can be further studied with Multi-level UPQC for micro-grid in distribution network as future work.

References

1. G. Vijayakumar , N. Gupta and R. A. Gupta, "Mitigation of power quality problems using shunt active power filters: A comprehensive review" 12th IEEE Conference on Industrial Electronics and Applications (ICIEA), 18-20 June 2017.
2. M. Kesler, and E. Ozdemir, "Synchronous-Reference-Frame-Based Control Method for UPQC under Unbalanced and Distorted Load Conditions", IEEE Transactions on Industrial Electronics, Vol. 58, No. 9, pp. 3967-3975, September 2011.
3. M. Suresh, and A. K Panda, "PI and Fuzzy Logic Controller based 3-phase 4-wire Shunt active filter for mitigation of Current harmonics with Id-Iq Control Strategy", Journal of power Electronics , Vol. 11, No. 6, pp. 914-921, Nov 2011.
4. S R. Das, P. K. Ray, A. Mohanty and G. Panda, "Power Quality Enhancement in PV and Battery Storage Based Microgrid Using Hybrid Active Filter" 2020 3rd International Conference on Energy, Power and Environment: Towards Clean Energy Technologies, 5-7 March 2021.
5. M. Suresh and A. K. Panda, "RTDS hardware implementation and simulation of SHAF for mitigation of harmonics using p-q control strategy with PI and Fuzzy logic controllers", Frontiers of Electrical and Electronic Engineering, Vol. 7, No. 4, pp. 427–437, Jun. 2012.
6. C.L. Hsiung, "Intelligent Neural Network-Based Fast Power System Harmonic Detection," IEEE Transactions on Industrial Electronics, Vol. 54, No. 1, pp. 43-52, Feb.2007.
7. P.K.Dash, S.K.Panda, T.H.Lee J.X.Xu and A.Rou tray, "Fuzzy and Neural Controllers for Dynamic Systems: an Overview". IEEE, May 1997.

8. S. Devassy, and B. Singh, "Design and Performance Analysis of Three-Phase Solar PV Integrated UPQC", ICPS, IEEE-March 2016.

9. V. K Krishna, S. K. Dash and K.R Geshma, "Development and Analysis of Power Quality by using Fuel cell based Shunt Active Power Filter", 2020 2nd International Conference on Innovative Mechanisms for Industry Applications (ICIMIA), 5-7 March 2020

10. A. Mishra, S. R. Das, P. K. Ray, R.K. Mallick, A. Mohanty and D. K. Mishra, "PSO-GWO Optimized Fractional Order PID Based Hybrid Shunt Active Power Filter for Power Quality Improvements" IEEE ACCESS, Vol. 8, pp. 74497 – 74512, April-2022.

11. K. Chandrasekaran, J. Selvaraj, C. R. Amaladoss and L. Veerapan, "Hybrid renewable energy based smart grid system for reactive power management and voltage profile enhancement using artificial neural network", Energy Sources, Part A: Recovery, Utilization, and Environmental Effects, Vol. 43, No. 19, pp. 2419–2442, March 2021.

12. M. R. Mohanraj and R. Prakash, "A Unified Power Quality Conditioner for Power Quality Improvement in Distributed Generation Network Using Adaptive Distributed Power Balanced Control (ADPBC)", International Journal of Wavelets, Multi-resolution and Information Processing, Vol. 18, No. 01, pp. 1941021, June 2020.

13. K. Sarker, D. Chatterjee and S. K. Goswami, "A modified PV-wind-PEMFCS-based hybrid UPQC system with combined DVR/STATCOM operation by harmonic compensation", International Journal of Modeling and Simulation, Vol.41, No.4, pp. 243-255, March 2020.

14. T. S. Saggu, L. Singh, B. Gill and O. P. Malik, "Effectiveness of UPQC in Mitigating Harmonics Generated by an Induction Furnace", Electrical power components and systems, Taylor & Francis, Vol. 46, No. 6, pp. 629-636, Nov-2018.

15. S.S. Dheeban and N.B. Muthu Selvan, "ANFIS-based Power Quality Improvement by Photovoltaic Integrated UPQC at Distribution System", IETE Journal of Research, Feb-2021.

16. S. Samal, and Hota, P.K, "Design and analysis of solar PV-fuel cell and wind energy based microgrid system for power quality improvement", Cogent Engineering, Vol.4,No.1, pp. 1-22, Nov-2017.

17. U. K. Renduchintala, C. Pang, K. M. Tatikonda, Yang, L,"ANFIS-fuzzy logic based UPQC in interconnected microgrid distribution systems: Modeling, simulation and implementation", The Journal of Engineering, Vol. 21, No.1, pp. 1-29, Feb-2021.

18. C. Pazhanimuthu, S. Ramesh, "Grid integration of renewable energy sources (RES) for power quality improvement using adaptive fuzzy logic controller based series hybrid active power filter (SHAPF)", Journal of Intelligent & Fuzzy Systems, Vol. 35, No. 1, pp. 749-766, July- 2018.

19. K. Srilakshmi, K.K.jyothi, and S.R. Surender, "Design of Multi-Objective-Based Artificial Intelligence Controller for Wind/Battery-Connected Shunt Active Power Filter", MDPI Algorithms, Vol. 15, No. 8, pp. 256, Aug-2022.

20. F. Ayadi; I. Colak; I. Garip, H. Bulbul, "Impacts of Renewable Energy Resources in Smart Grid", 8th International Conference on Smart Grid, Paris, pp. 183-188, June 2020.

21. I. Colak; R. Bayindir, S. Sagiroglu, "The Effects of the Smart Grid System on the National Grids", 8th International Conference on Smart Grid, Paris, pp. 122-126, June 2020.

22. S. Jaber, A. M. Shakir, "Design and Simulation of a Boost-Microinverter for Optimized Photovoltaic System Performance", International Journal of Smart Grid, Vol. 5, No. 2, pp. 1-9, June 2021.

23. S. Ikeda, F. Kurokawa, "Isolated and wide input ranged boost full bridge DC-DC converter for improved resilience of renewable energy systems", San Diego, CA, USA, pp. 290-295, 5-8 Nov. 2017.

24. S. S. Dash, "Tutorial 1: Opportunities and challenges of integrating renewable energy sources in smart" 6th International Conference on Renewable Energy Research and Applications, San Diego, CA, USA, 5-8 Nov. 2017.

25. M. Tsai, C. Chu, W. Chen, "Implementation of a Serial AC/DC Converter with Modular Control Technology", 7th International Conference on Renewable Energy Research and Applications, Paris, France, pp. 245-250, Oct. 2018.

26. A. Thakallapelli, S. Ghosh; S. Kamalasadan, "Real-time frequency based reduced order modeling of large power grid" IEEE Power and Energy Society General Meeting Boston, MA, USA, 17-21 July 2016.

27. A. Belkaid, I. Colak, K. Kayisli, R. Bayindir, Improving PV System Performance Using High Efficiency Fuzzy Logic Control, 8th International Conference on Smart Grid, Paris, pp.152-156, June 2020.

28. K. Srilakshmi, N. Srinivas, P. K. Balachandran, J.G.P. Reddy, S. Gaddameedhi, N. Valluri, S. Selvarajan, "Design of Soccer League Optimization Based Hybrid Controller for Solar-Battery Integrated UPQC", IEEE Access, Vol. 10, pp. 107116-107136, Oct-2022.

29. K. Srilakshmi, C. N. Sujatha, P. K. Balachandran, L. Mihet-Popa, and N. U. Kumar, "Optimal Design of an Artificial Intelligence Controller for Solar-Battery Integrated UPQC in Three Phase Distribution Networks", Sustainability, Vol. 14, No. 21, Oct-2022.